DOI 10.1007/s10556-020-00809-5
Chemical and Petroleum Engineering, Vol. 56, Nos. 7-8, October, 2020 (Russian Original Nos. 7-8, July–August, 2020)

SAFETY. DIAGNOSTICS. MAINTENANCE

ASSESSMENT OF CONDITIONS FOR DETECTING CORROSION CRACKING OF WELDED JOINTS BY ACOUSTIC EMISSION METHOD*

I. A. Rastegaev,[1] I. I. Rastegaeva,[1] D. L. Merson,[1] and A. V. Chugunov[2]

UDC 620.165.2:620.162.4:620.179.17

The analysis of acoustic emission (AE) signs of the early development of corrosion cracking of a welded joint is carried out on the example of real data of technical diagnostics of a butane heater of a gas fractionation unit obtained using the AE method before and after eliminating the defect. The possibility and conditions of detecting the designated defect were studied using five basic criteria for assessing the degree of hazard of AE sources: amplitude, integral, local dynamic, integral dynamic, and the MONPAC criteria. For all these AE criteria, the values of empirical coefficients that ensure the detection of a defect of this type were determined, and the dynamics of the defect development in the coordinates of the estimated parameters was established. The organizational and technical requirements that increase the likelihood of detecting corrosion damage during AE control are described.

Keywords: non-destructive testing, metal corrosion cracking, acoustic emission, hazard criteria.

Metal corrosion damage of technological equipment of chemical, oil and gas processing industries is divided into a large number of types and subtypes depending on the metal properties, the operation environment and the conditions of their interaction [1].

Revealing and assessing the hazard of corrosion damage is a relevant issue of diagnosing and forecasting the equipment life.

One of the methods of non-destructive testing (NDT) for detecting corrosion damage is the method of acoustic emission (AE) [2].

Since the AE method is at the industrial approbation stage now [2], there are no recommendations for its application in regulatory documents and literature sources, for example: how to detect a defect using AE data; how to adjust the AE equipment to ensure sensitivity to a defect; which assessment criteria to use and which values of empirical parameters and coefficients need to be set, etc. Laboratory results of diagnostics of metals corrosion damage are not directly suitable for practical use, and similar data (with no less scientific novelty), established in practice, accumulate slowly (since they are rare events) and are hardly available (they are the experience of laboratories and are practically not published); these facts significantly hinder the development of the AE method and the regulatory framework for its application.

* The results of steel St3 tests, obtained during the implementation of project No. RFMEFI57714X0145, were partially used in the study.

[1] Togliatti State University, Togliatti, Russia; email: RastIgAev@yandex.ru.

[2] Profil' Ltd, Togliatti, Russia.

Translated from Khimicheskoe i Neftegazovoe Mashinostroenie, Vol. 56, No. 7, pp. 24–29, July, 2020.

 0009-2355/20/0708–0554

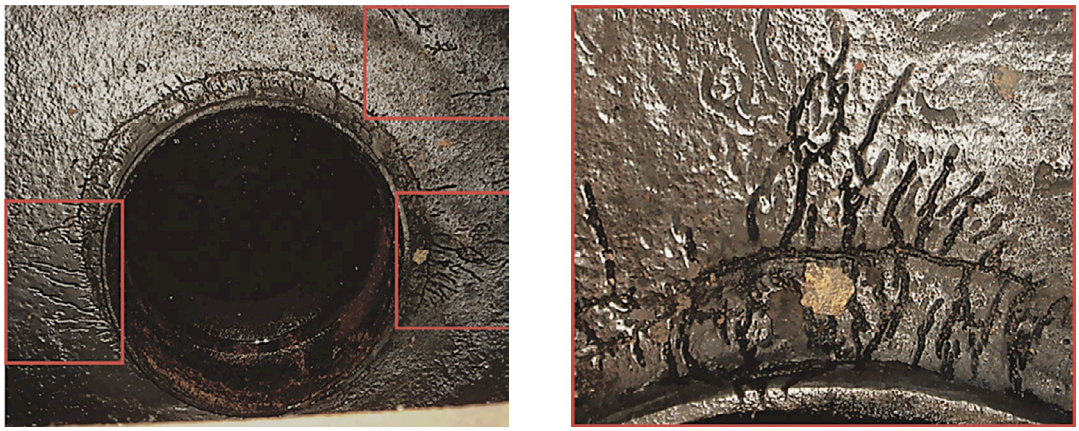

(a) (b)

Fig. 1. Photo of the weld of the butane heater fitting welding with corrosion damage (a) and an enlarged fragment of the photo (b).

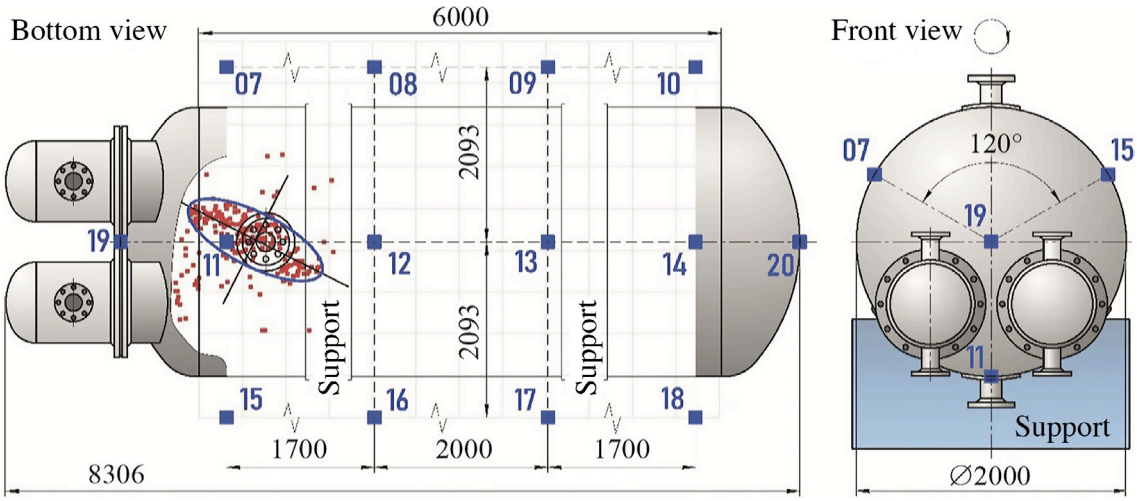

Fig. 2. Monitored object with an overlaid fragment of the location map: AE event; 11 Location and number of the AE transducer.

This study is based on the results obtained in the diagnostics of a real industrial facility using a scientific-research approach, which made it possible to formulate AE signs of a defect, to establish the limits of the AE method applicability and the values of empirical coefficients for the assessment criteria of the defect hazard rate, which are currently adopted [3–6].

This material can be useful for specialists using the AE method for detecting corrosion damage.

The subject of research is the assessment by the AE method of the conditions for detecting damage of welded joints associated with corrosion cracking at the boundaries of fusion of the weld with the base metal during a typical test of capacitive equipment for strength and density.

The object of research is corrosion damage of a welded joint of the fitting welding (Fig. 1), revealed during an internal examination in the lower generating line of the butane heater (Fig. 2) of the gas fractionation unit of the oil refinery. This example is demonstrative, since according to the results of the complete visual and ultrasonic examination, no other corrosion damage of the heater was revealed, i.e, the difference between the AE signals

recorded before and after the defect elimination is related exactly to this defect, i.e. this difference in the AE data can be considered specific for all defects of this type.

The heater is a horizontal vessel with elliptical bottoms, in which, by means of two U-shaped tube banks, butane is heated to a temperature of 225 ± 25 °C at a pressure of 0.8 MPa.

The heater shell (see Fig. 2) with overall dimensions of $\varnothing 2.0 * 7.2$ m is made of St3 GOST 380 sheet steel 20 mm thick.

The service life of the heater at the time of the AE testing was 47 years.

The AE testing of the heater before the defect repair revealed the presence of an acoustic emission source with localization in the area of the defective fitting (see Fig. 2).

The corrosion damage looks like smooth annular grooves up to 2 mm deep, up to 4 mm wide, clearly tracing the boundaries of fusion of the weld with the base metal of the shell and the fitting around the circumference. The annular grooves are connected by analogous radial grooves that run in the spaces between the beads of the weld (see Fig. 1).

On the base metal of the fitting, no such damage was revealed, but on the base metal of the vessel shell near the fitting, three small areas with a similar damage were observed (see Fig. 1).

In other parts of the shell (including welded joints of the cylinder shell and welding of fittings along the upper generating line of the vessel), no such damage was found on the inner and outer sides.

Visually, no cracks were observed in the grooves. However, during mechanical sampling of metal damage followed by liquid penetrant testing, shallow surface cracks were found in the grooves, which indicates an early stage of defect development. Despite this, the repair (replacement of the fitting) was carried out and was followed by two tests of the vessel: the first test was for relaxation of welding stresses [2], the second was a control test for recording and assessing the AE. During the control test after repair, neither active nor localized AE sources were found (results are not given); therefore, acoustic emission registered before repair is associated with the investigated defect.

Equipment and Research Technique

The AE studies were performed according to the method [3] during hydraulic tests of the heater.

Water was supplied to the vessel fitting, located on the upper generating line (closer to the bottom, as far as possible from the defective area).

Loading diagram of the vessel consisted of three stages: holding for 10 min at a pressure of 0.5 MPa; holding for 10 minutes at a pressure of 0.8 MPa; holding for 5 minutes at a pressure of 1.1 MPa (lower than the test pressure by 13 %).

AE was taken from the object through the Litol-24 contact medium with R15I-AST piezoelectric transducers (resonance frequency of 150 kHz) and recorded by the PAC DiSP-SAMOS 24 system (Physical Acoustics Corporation) with the following settings: frequency range of 0.1–0.4 MHz, overall gain of 40 dB, discrimination threshold of 30 dB (fixed), hit definition time (HDT) of 800 μs, hit lockout time (HLT) of 1000 μs, peak definition time (PDT) of 200 μs. The actual average group velocity of the acoustic pulse propagation in the heater shell was $C_m = 3.35$ km/s, which at the control frequencies corresponds to contention scope of the three Lamb waves modes: A0, A1, S1 (it was determined by the dispersion curves calculated for "water/steel 20 mm/air, +25 °C" boundary conditions in the PACshare Dispersion Curves software package).

The ambient acoustic noise at the test object did not exceed 25 dB, the actual decay rate was $\delta = 5.1$ dB/m. To simulate the AE when adjusting the equipment, Hsu–Nielsen source was used [3, 7].

The layout of the acoustic emission transducers (AET) and the location map are shown in Fig. 2, the results of AE testing are shown in Fig. 3.

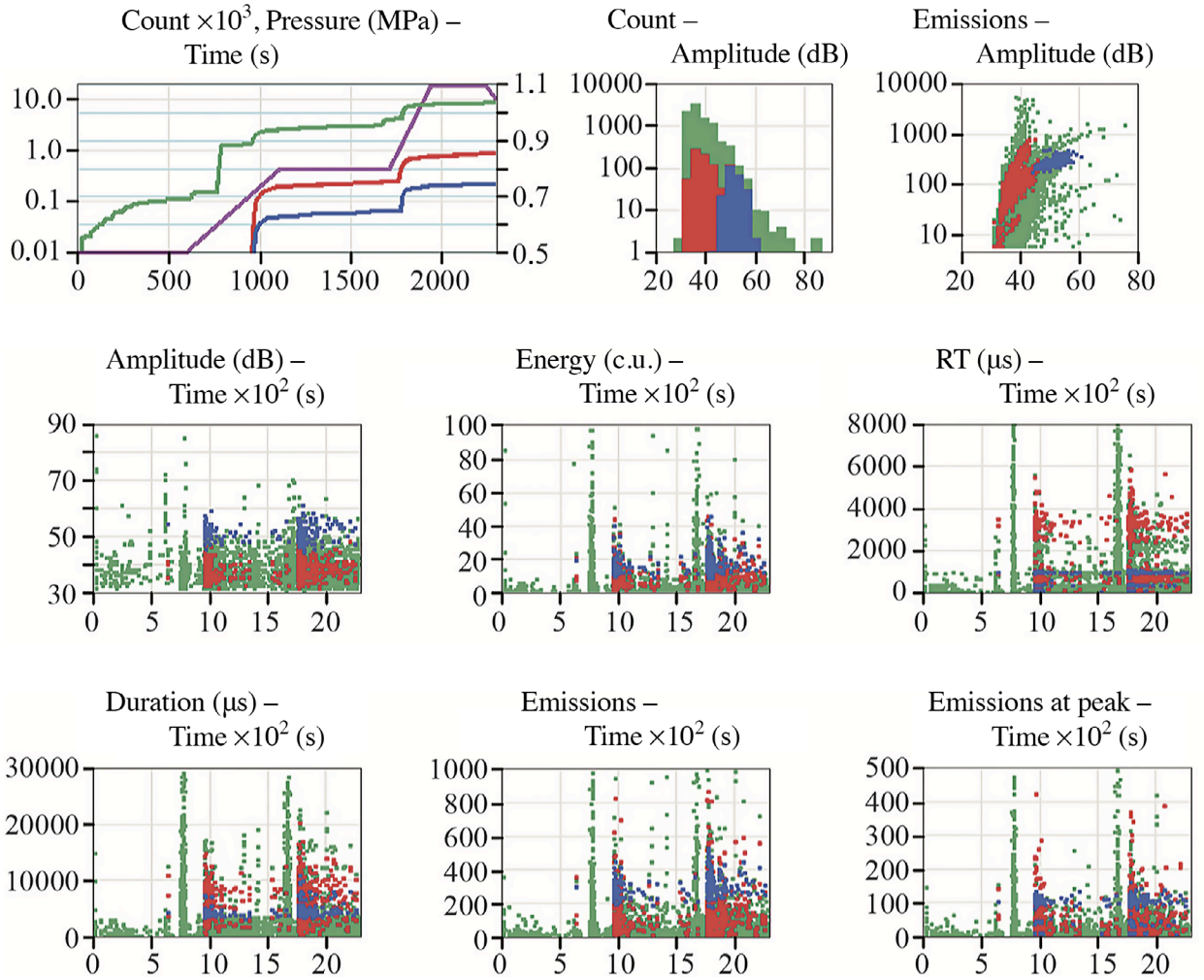

Fig. 3. Graphs of AE parametric distributions: Green — all signals recorded during the test; Red — location signals from AET No. 7, 8, 11, 12, 15 and 16; Blue — location signals from AET No. 11; Purple — loading diagram.

Investigation Results and Their Discussion

Corrosion damage was explicitly seen on the location map (see Fig. 2), while corrosion products were not detected, and damages in the form of grooves are not significant stress concentrators to manifest themselves as an active AE source [2].

It indicates that the AE coherently detected by several channels is associated with corrosion cracking of the material.

To separate these signals, the AE signals included in the location events (see Fig. 3, Red and Blue) are superimposed on the parametric graphs of the entire detected AE (see Fig. 3, Green). Signals detected by distant AETs (No. 7, 8, 12, 15, 16) are highlighted in red in order to visualize the influence of transformation and decay on the distortion of the estimated AE parameters in relation to the signals highlighted in blue, detected by the closest to the defect AET No. 11 with minimal distortions.

It is known [2] that according to the features of the signal shape in the parameters "number of emissions — amplitude", it is possible to separate the "true" AE signals from noise. From the corresponding graph (see Fig. 3),

it is obvious that the signals included in the location events are not interference and lie in the area of the "true" AE signals [2]. The range of changes in the AE activity during the test did not exceed 2.5 pulses/s for location events and 5 pulses/s for all AE signals detected by AET No. 11. At that, the maximum of the AE activity fell on the loading stages, which indicates low AE generation rate of the source.

In the near-field zone from the source (the distance from the defect to AET No. 11 $\Delta x_{11} \approx 0.3$ m), AE signals in amplitude are in the range of 45–60 dB with a maximum of 51 dB and are compactly distributed in the temporal estimated parameters which characterize the signal shape (rise time (RT); duration; total number of emissions; number of emissions at peak of the amplitude).

In the far-field zone from the source (the distance from the defect to AET No. 8 or 16 $\Delta x_{08} \approx 2.2$ m), due to the decay, the same signals are distributed in amplitude in the range of 30–45 dB with a maximum of 37 dB, and as a result of the transformations of their shapes, the spread of temporal estimated parameters is wider.

It should be emphasized that when analyzing the entire set of detected AE signals (see Fig. 3, green color), the defect does not appear in any of the considered coordinates of the AE assessment. It means that when determining the hazard class of an AE source of a certain type, it is always necessary to assign the location clusters and bring the estimated parameters of the signals included in the cluster to the location of the source, i.e. take into account the decay and distortion of signals.

Consequently, when searching for a defect of a certain type, it is unacceptable to overly minimize the number of antenna groups and carry out monitoring at their sensitivity limit (i.e. at the maximum distance between AETs).

Using the signals included in the location events and detected by AET No. 11 (as the least distorted), it is possible to back-calculate the values of empirical parameters and coefficients that determine the effectiveness of the application of the following AE criteria: amplitude, local dynamic, integral, integral dynamic, and the MONPAC criterion [3–6]. For definiteness, the source hazard classes are accepted: III according to [3, 5] and *C* according to [6], according to which the results of AE monitoring should be verified by other NDT methods. It is necessary to standardize the conditions for mandatory confirmation and measurement of a corrosion defect, which is, although a surface damage, but of a crack-like type, which means it is subject to further development.

The amplitude criterion consists in comparing the average amplitude of AE events (A_{av}) with the permissible amplitude (A_t). At that, the AE source will have the III hazard class in case of $A_{\text{av}} > A_t$ [2–4, 8]. Taking all the empirical coefficients of the amplitude criterion equal to 1 (which is allowed according to [3] and [2, 8]) and solving the inverse problem taking decay into account, one obtains:

$$A_t = A_{\min} + \delta \cdot \Delta x_{11} = 45\text{dB} + 5.1\text{dB/m} \cdot 0.3\text{m} = 46.5\text{dB},$$

where $A_{\min}$ is the amplitude threshold of crack formation [8] (taken as the lower boundary value of the distribution range of amplitudes detected by AET No. 11).

The result obtained agrees with the experimental data of fatigue testing of a welded joint made of St3 (Fig. 4a) with its destruction in the heat-affected zone (HAZ) weakened by stress concentrators, as well as with the data of [9]. The results (see Fig. 4a) were obtained on test equipment and under the conditions described in [10].

The integral criterion consists in the interval comparison of the average activity of the AE source F with its relative strength J_k [3, 4, 8], which are defined as

$$F = \frac{1}{K} \cdot \sum_{k=1}^{K} \frac{N_{k+1}}{N_k}, \tag{1}$$

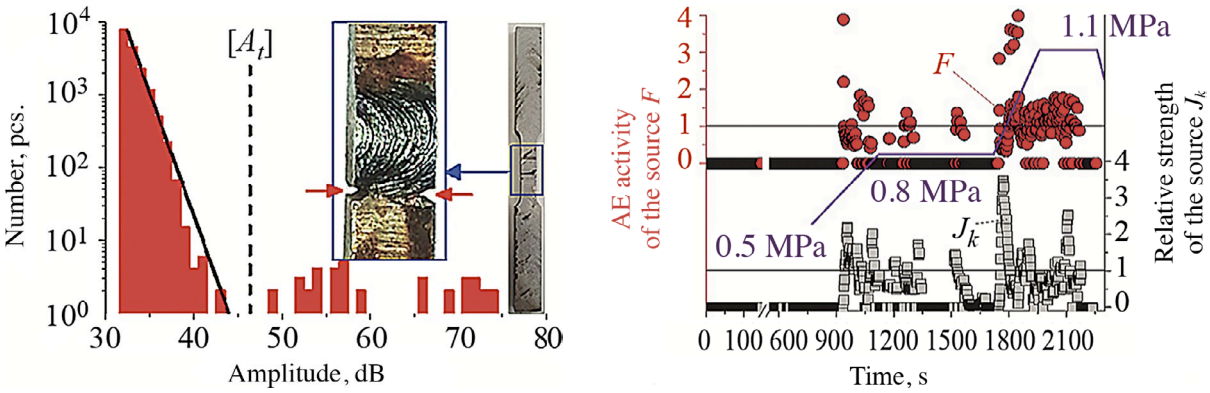

Fig. 4. Diagram of the AE amplitude distribution obtained during fatigue testing of the St3 welded joint with a notch in the HAZ (a) [10] and the results of interval calculation of the estimated parameters of the integral criterion (b).

$$J_k = \frac{A_k}{wA_m}, \tag{2}$$

where N_k, N_{k+1} are the numbers of events in the k th and $(k+1)$th intervals of the parameter estimation $(k = 1,2 \ldots K)$; K is the total number of estimation intervals; A_k, A_m are the average amplitudes of the AE source in the interval k and in the interval $m = (K - k)$, respectively, dB; w is the empirical coefficient.

Since in [3, 4, 8] there are no recommendations on the choice of k, K, w, their values were obtained as a result of iterations of calculating the hazard degree until the source corresponds to class III (according to the condition $F > 1$ at $J_k < 1$ and $J_k > 1$ [3, 4]). The result of calculating F and J_k by a sliding window 80 s long, which is divided into intervals of 20 s, corresponds to this condition, i.e. in Eq. (1), the values of the parameters are: $k = 20$ s, $K = 80$ s with a calculation step (window shift) of 2 s, in Eq. (2), $w = 0.25$ (see Fig. 4b).

The integral dynamic criterion is implemented only for localized AE sources [3, 5], for which parameters that take into account the concentration of locations C, their energy E and the dynamics of energy release U are determined according to the following formulas:

$$C = \frac{1}{R_L^2} \cdot \sum_{l=1}^{L} Z_l, \tag{3}$$

$$E = \sum_{l=1}^{L} A_l^2 \cdot N_l, \tag{4}$$

$$U = \frac{\sum_{l=1}^{L} l \cdot (A_{l+1}/A_l)^2}{\sum_{l=1}^{L} l}, \tag{5}$$

where Z_l is the location event No. l, $l = 1,2,\ldots,L$; L is the number of events under consideration in the order

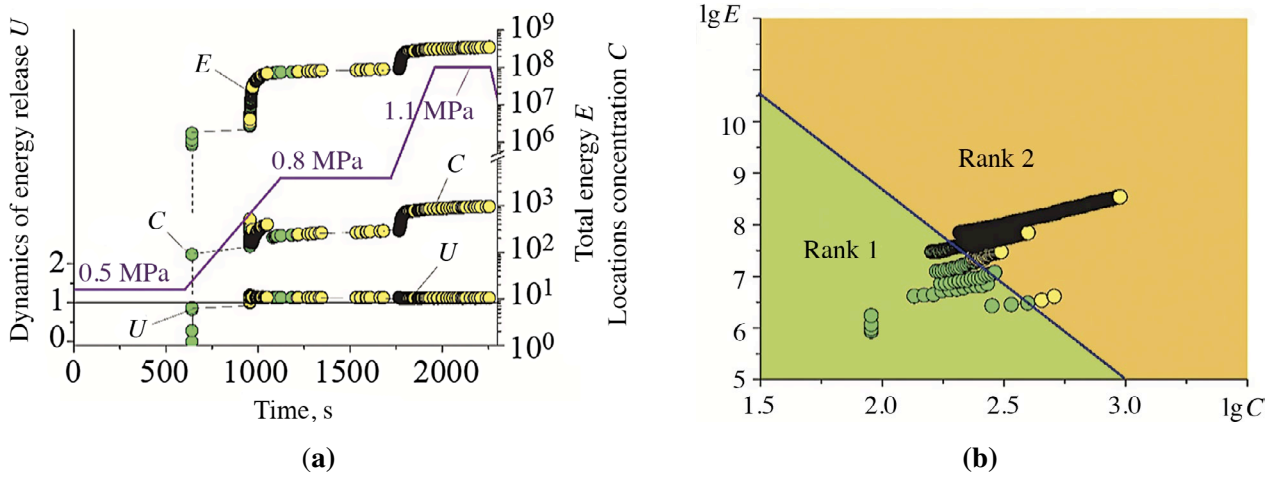

(a) (b)

Fig. 5. Results of calculating the estimated parameters of the integral dynamic criterion, presented over the time of AE registration (a) and in mutual coordinates (b).

of their registration; N_l is the number of emissions in the location event No. l; A_l, A_{l+1} are the amplitudes of location event No. l and the following event No. $(l+1)$, dB; R_L is the average radius of the AE source location cluster at the moment L, m. The R_L value is defined as the radius of a circle inscribed in the location cluster, bounded by the scattering ellipse. The principal axes of the ellipse, onto which the location events were projected later, were determined by the Principle Component Analysis [11, 12]. The boundaries of the scattering ellipse are set equal to $\mu \pm 2\sigma$ of the probability density of the distribution of data projections on the principal axes (μ is the mathematical mean value, σ is the root-mean-square deviation). Parameters C, E, U were calculated continuously in accordance with data accumulation from the beginning $(l = 1,\ L = 1)$ to the end $(l = 1,\ L = \max)$ of the test (Fig. 5).

In Fig. 2, as an example, the principal components and the scattering ellipse obtained from all location events are plotted.

According to Fig. 5a, starting from the middle of the stage of loading the vessel with a pressure of up to 0.8 MPa, the parameter of the dynamics of the AE energy release $U \approx 1.1-1.2$, which, according to [3, 5], allows the source to be assigned to 4th type $(U > 1)$. Therefore, in order to correspond the AE source to the III hazard class, the source's rank should be equal to 2 [3, 5]. The boundaries of the ranks on the $\lg C$–$\lg E$ plane (see Fig. 5b), the values of which are empirically determined according to [3, 5], correspond to this condition.

The MONPAC criterion is based on the principle of zone location (Zonal Intensity Processing) with subsequent classification of AE sources in two-parameter coordinates of the strength S and historical H indices [6]. The S and H values were calculated for all AE signals registered by AET No. 11 for the entire test period as

$$S(t) = \frac{1}{10} \cdot \sum_{y=1}^{y=10} G_y^{\max}(t, 0 < t < D), \tag{6}$$

$$H(t) = \frac{D}{(D-d)} \cdot \frac{\sum_{i=d+1}^{D} G_i(t)}{\sum_{i=1}^{D} G_i(t)}, \tag{7}$$

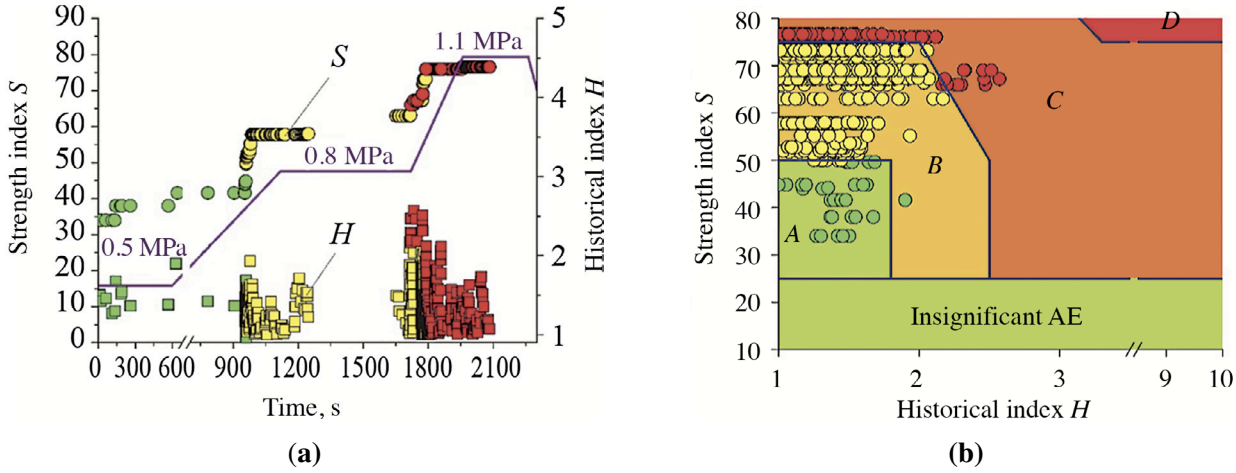

Fig. 6. Results of calculating the estimated parameters of the MONPAC criterion, presented over the time of AE registration (a) and in mutual coordinates (b).

where $G_i(t)$ is the strength of the ith AE signal (doubled area under the envelope of the AE signal), $i = 1, 2, \ldots, D$; D is the interval of the total count (number of signals), on which the calculation of S and H is carried out; $G_y^{\max}(t)$ is one of ten signals $(y = 1, 2, \ldots, 10)$ having maximum values of the strength $G^{\max}$ on the calculated interval D (the selection of ten signals with $G^{\max}$ is a mandatory requirement according to [6], but not regulated by [3] and other regulatory documents); $(D - d)$ is the size of the sliding calculation window H; d is an empirical factor that depends on the total number of accumulated signals.

The calculation of S and H was carried out sequentially from the beginning of the test to the observation point D with a window $(D - d) = 5$ and a window shift step of 1 signal. Initial calculated point $D_{\min} = 50$ signals. The calculation was also carried out in several iterations with a change in the size of the sliding window $(D - d)$ until the defect obtained compliance with the AE hazard criterion of class III (which, according to [6], corresponds to class C). Before calculating S and H, the Swansong filter [6] was applied. The final calculation results for the investigated defect and the loading diagram are shown in Fig. 6.

The local dynamic criterion [3, 4] (or *the Dunegan–Ivanov–Bykov criterion* [2, 8]) consists in determining the degree m, which reflects the increments in the total AE count ΔN_i per load unit ΔP_i:

$$m = \frac{\Delta N_i \cdot P_i}{N_i \cdot \Delta P_i}, \tag{8}$$

where $\Delta N_i = N_{i+1} - N$, $\Delta P_i = P_{i+1} - P$; N_{i+1} and P_{i+1}, N_i and P_i are the number of emissions and the load value in the next $(i+1)$th and previous ith events, respectively.

A prerequisite for the adequate application of this criterion is the parallel registration of the load by a pressure sensor, which was not done in this study. The loading diagram is compiled according to the time marks of the beginning/end of pressure rise, the pressure was recorded by a indicating pressure gauge (see Fig. 3, Parametric 1); therefore, the time marks of ΔP_i were not synchronized with ΔN_i. In this regard, according to the available data, it is not possible to adequately trace the manifestation of the investigated AE source in the m–time coordinates. However, an integral estimate of m is possible by the marks of the beginnings (i) and ends $(i+1)$ of loading stages. Such an assessment was made for the second stage of loading, at which (according to calculations using other AE criteria) the defect manifested itself as much as possible.

The largest value of m was 1.9 (class III) when calculating according to all AE data, 6.5 (IV class) when calculating according to location data, 5.9 (class III) when calculating according to AE signals detected only by AET No. 11. Despite the positive result, this assessment should be considered approximate; nevertheless, it is possible to make a conclusion that a more "strict" assessment was obtained in the calculation based on the location data.

CONCLUSIONS

A defect (damage) of the welded joint by the mechanism of corrosion cracking, which is at an early stage of development, generates AE of low activity and amplitude. Therefore, the probability of missing such a defect is high when assessing the hazard degree of defects over the entire data array obtained during AE testing (over all channels). To increase the likelihood of detecting a defect, it is advisable to determine the class of its hazard only by the AE parameters of events included in the location clusters formed by the antenna groups closest to the AE source (defect). Therefore, when searching for a defect, it is not recommended to overly minimize the number of antenna groups and carry out AE monitoring at the sensitivity limit of the sensors. The obtained results have confirmed that if these conditions are met and the values of empirical coefficients established in the study are applied, corrosion cracking can be detected by all the main AE criteria used today. At that, the amplitude criterion has the least dependence on empirical coefficients.

According to the authors of this article, in order to increase the likelihood of detecting a defect during monitoring, it is advisable to classify the hazard degree of AE sources with the parallel application of several criteria; the requirement for rechecking all locations by additional methods of non-destructive testing, starting with hazard class II, should be mandatory, not advisory [3].

REFERENCES

1. N. A. Gafarov, A. A. Goncharov, and V. M. Kushnarenko, *Determination of Reliability Characteristics and Technical Condition Performances for the Equipment at Sour Oil and Gas Fields* [in Russian], Nedra, Moscow (2001).
2. V. I. Ivanov and V. A. Barat, *Acoustic Emission Diagnostics: Handbook* [in Russian], Spektr, Moscow (2017).
3. PB 03–593–03, *Rules for Organizing and Performing Acoustic Emission Control of Vessels, Apparatuses, Boilers and Industrial Pipelines* [in Russian], Promyshlennaya Bezopasnost', Moscow (2004).
4. Z. Nazarchuk, V. Skalskyi, and O. Serhiyenko, *Acoustic Emission. Foundations of Engineering Mechanics*, Springer, Cham (2017).
5. NDIS 2412–80, *Acoustic Emission Testing of Spherical Pressure Vessel Made of High Tensile Strength Steel and Classification of Test Results, Japanese Society for NDI* (1980).
6. T. J. Fowler, J. A. Blessing, P. J. Conlisk, and T. L. Swanson, "*The MONPAC system*," *J. Acoust. Emis.*, **8**, No. 3, 1–8 (1989).
7. M. G. R. Sause, "*Investigation of pencil-lead breaks as acoustic emission sources*," *J. Acoust. Emis.*, **29**, 184–196 (2011).
8. V. V. Klyuev (ed.), V. I. Ivanov, G. A. Bigus, and I. E. Vlasov, *Acoustic Emission: Textbook* [in Russian], Spektr, Moscow (2011).
9. V. V. Murav'ev, M. V. Murav'ev, and S. A. Bekher, "*Effect of loading conditions on informative parameters and signal spectra of acoustic emission in samples of carbon steels*," *Russ. J. Nondestruct. Test.*, **38**, No. 7, 483–492 (2002).
10. I. A. Rastegaev, M. L. Linderov, D. L. Merson, et al., "*Monitoring of fracture of welded joints in hazardous facilities by acoustic emission under static and cyclic loadings*," *Indian J. Sci. Technol.*, **8**, No. 36, 90555 (2015).
11. I. T. Jolliffe, *Principal Component Analysis. Springer Series in Statistics*, Springer, New York (2002).
12. H. Abdi and L. Williams, "Principal component analysis," *WIRes Comput. Stat.*, **2**, No. 4, 433–459 (2010).